JOURNAL OF GEOPHYSICAL RESEARCH, VOL. 115, C03005, doi:10.1029/2009JC005574, 2010

Modality of semiannual to multidecadal oscillations in global sea surface temperature variability

Ge Chen,[1,2] Baomin Shao,[1,2] Yong Han,[1,2] Jun Ma,[1,2] and Bertrand Chapron[3]

Received 15 June 2009; revised 29 September 2009; accepted 1 October 2009; published 3 March 2010.

[1] Repeating the history of study on El Niño-Southern Oscillation (ENSO) in the 1980s, interdecadal oscillation (IDO) in climate variability is currently an area of active research and debate, following the recognition of its emerging significance in nature and science. In this work, a two-dimensional propagating modal extraction technique is applied to a reconstructed global monthly sea surface temperature (SST) data set spanning 1854 through 2007, to examine the spatiotemporal structure of SST variability with an emphasis on the fine modal pattern of IDOs. In the time domain, it is revealed that a canonical modal spectrum of decadal-to-centennial SST variability constitutes four most distinct oscillations with periodicities at 9.0, 13.0, 21.2, and 62.2 years, which are naturally defined as primary modes and are, respectively, termed as the subdecadal mode, the quasidecadal mode, the interdecadal mode, and the multidecadal mode (modes S, Q, I, and M). They join the energetic annual mode (mode A) and two major ENSO modes at 3.7 and 5.8 years (modes B and C), as well as a dozen of secondary modes ranging from semiannual to multidecadal, in determining the key pattern of SST-related climate variability. In the space domain, seven modally dynamic areas, analogous to the Niño regions for ENSO, are clearly identified and are named as IDO zones. Contrary to ENSO, dominant IDO zones are most visible in the extratropical oceans, especially in the North Atlantic/North Pacific sectors, while secondary signatures are observed in the tropical oceans. The array of (four) primary modes with respect to (seven) major zones yields a sophisticated yet canonical pattern of IDOs, leading to a basic conclusion that multimodality (for a given region) and multiregionality (for a given mode) are fundamental features of the IDO system.

Citation: Chen, G., B. Shao, Y. Han, J. Ma, and B. Chapron (2010), Modality of semiannual to multidecadal oscillations in global sea surface temperature variability, *J. Geophys. Res.*, *115*, C03005, doi:10.1029/2009JC005574.

1. Introduction

[2] Sea surface temperature (SST) has been intensely used by both the oceanographic and the meteorological communities as a result of its tremendous scientific importance attached to ocean/atmosphere thermodynamics, air-sea interaction and global climate change, and its observational availability from various field and remote sensing instruments. Two main categories of climatological SST data have become available during the past decade: In situ-based medium resolution (1°–5°) centennial data set [e.g., *Rayner et al.*, 2006; *Smith et al.*, 2008], and satellite-based high-resolution (1–10 km) decadal data set [e.g., *Vazquez et al.*, 1998; *O'Carroll et al.*, 2006]. The former category has reconstructed a monthly time series longer than 1.5 centuries, while the latter has accumulated an over two decade time series on daily basis.

[3] The current duration and resolution of existing climatological data sets allow a suite of natural modes in SST variability to be extracted (for a brief review, see *Chen and Li* [2008]). The identified modes of SST variability at timescales from seasonal to centennial can be grouped into three regimes: The annual regime (1–18 months), the interannual regime (1.5–8 years), and the interdecadal regime (8–100 years). Obviously, satellite data are superior in resolving high-frequency signals in the annual regime, while reconstructed data are advantageous in recovering low-frequency oscillations in the interdecadal regime. The SST modes in the interannual regime, known as the El Niño-Southern Oscillation (ENSO) band, are within the resolvable frequencies of both kinds of data, and can thus serve as a common ground for comparison of the two data sources.

[4] In addition to data set itself, the identified SST modes are also subject, and sometimes sensitive, to extracting techniques employed. In most of the previous investigations, the prevailing principal component analysis (PCA) methods, such as empirical orthogonal function (EOF) and singular value decomposition (SVD) or their variations, are used (see Table 2 of *Chen and Li* [2008]). As an alternative, a recently proposed two-dimensional propagating modal extraction scheme is also applied [*Chen*, 2006], showing notable success in identifying fine patterns of ENSO modes.

[1] Engineering Research Center of Marine Information Technology, Ministry of Education, Qingdao, China.
[2] Department of Marine Technology, College of Information Science and Engineering, Ocean University of China, Qingdao, China.
[3] Department of Physical and Space Oceanography, IFREMER, Plouzané, France.

0148-0227/10/2009JC005574$09.00

[5] On the basis of accumulating data and evolving techniques, the history of study on ENSO in the 1980s is being repeated with that on interdecadal oscillation (IDO) in climate variability over the past two decades, following the recognition of its emerging impact on natural environment and close relevance to human life. Tremendous efforts have been devoted to describing the characteristics and explaining the mechanisms of IDO-related SST variabilities. Among them, the Pacific decadal oscillation (PDO), which represents a special class of Pacific decadal variability (PDV), defined by a preferred spatial pattern with a range of interdecadal timescales [*Mantua et al.*, 1997], draws perhaps the most intensive attentions by the research community. Despite that, descriptions of the PDO characteristics are crude and diverse among various authors, and the mechanisms for PDO behavior remain mysterious (see *Mantua and Hare* [2002] for a review). For example, what can be said about PDO frequency is that in the 20th century its fluctuations are most energetic in two broad periodicities: One from 15 to 25 years, and the other from 50 to 70 years. In terms of its physical mechanism, the three most likely hypotheses that have been proposed are ocean-atmosphere interaction, tropical-extratropical interaction, and internal tropical dynamics. Although the PDO mode of SST variability has been discussed widely in the literature, much controversy still exists over how it works, and how it might be best monitored, modeled, and predicted. Meanwhile, the more general quest for understanding PDV is also an area of growing concern and active debate. As pointed out by *Mantua and Hare* [2002] in their review article, one important lesson to learn from the numerous publications is that different analyses yield different descriptions of 20th century PDV, not to mention those concerning the interdecadal changes of other world's oceans.

[6] In view of the complexity of SST-related interdecadal variabilities on both global and regional scales, the main objective of this study is to provide a new (and hopefully more realistic) image of the spatiotemporal pattern of seasonal-to-centennial modes using our proposed scheme together with an up-to-date data set. In doing so, it is helpful to introduce two generalized abbreviations as extensions to the commonly used PDV and PDO: IDV and IDO, which stand for interdecadal variability and interdecadal oscillation, without referring to any specific ocean. The rest of this paper is organized as follows: The SST data used in our analysis are described along with a brief explanation of the adopted modal extraction scheme in section 2. The principal modes in SST variability are derived and characterized in section 3. The dominant IDO zones in the world's oceans are identified and presented in section 4. The detailed spatiotemporal patterns of natural SST modes and oscillations are revealed and analyzed in section 5. Our results are compared to relevant ones in the literature and are discussed in terms of physical mechanism in section 6. Finally, a summary with conclusions is given in section 7.

2. Data and Methodology

[7] The SST data used in this study are extracted from an extended reconstructed sea surface temperature (ERSST) product (Version 3) released by NOAA National Climatic Data Center [*Smith et al.*, 2008]. The ERSST product is generated on the basis of either Comprehensive Ocean Atmosphere Data Set (COADS) [*Woodruff et al.*, 1998] or International COADS (ICOADS) [*Worley et al.*, 2005] SST anomalies for its Version 1 and Versions 2–3, respectively. The SST data set extracted from ERSST Version 3 for this study is a monthly record with a global coverage at $2^\circ \times 2^\circ$ grids for the period of January 1854 through December 2007 (for details of the reconstruction analysis, the readers are referred to *Smith et al.* [2008], and references therein). The availability of an unprecedented over-1.5-century-long monthly SST data set allows, in theory, for a complete recovery of seasonal-to-multidecadal modes, meanwhile a preliminary identification of centennial trends.

[8] The main technique that will be used in this analysis is a recently designed fine mode extraction scheme [*Chen*, 2006]. A space-time data set documenting the global or regional variation of a geophysical quantity can be treated as a three-dimensional array: $D = D\{x_i, y_j, t_k\}$, with i, j, and k being integers and $1 \le i \le I$, $1 \le j \le J$, $1 \le k \le K$. Our scheme for extracting the principal modes from array D includes basically three steps: First, creating a detrended anomaly field, d, by taking out the annual means and trends from array D on point basis: $d = d\{x_i, y_j, t_k\}$; second, performing a harmonic analysis with a period T_n for each geographical location (x_i, y_j) (corresponding to longitude and latitude) on the basis of the time series $\{d_{t_1}, d_{t_2}, \ldots, d_{t_K}\}$, where n is an integer with $1 < n \le N$ and $T_N \le t_K$; third, the harmonic analysis is repeated $I \times J \times (N-1)$ times for $1 \le i \le I$, $1 \le j \le J$, and $1 < n \le N$, resulting in two three-dimensional arrays corresponding to amplitude and phase, respectively, $A = A\{x_i, y_j, T_n\}$, $P = P\{x_i, y_j, T_n\}$. Given its searching nature, no prior knowledge or assumption on data or mode property is needed, or, in other words, it is considered to be fully data adaptive. Combined analysis of A and P information allows a complete recovery of the intrinsic modes as a function of space and period within a resolvable band.

[9] Some form of significance test is needed to determine if the principal modes obtained by using the above scheme can be distinguished from those produced from a spatially and temporally uncorrelated random process. To do so, an evaluation technique based on Monte Carlo simulation proposed by *Overland and Preisendorfer* [1982] is adopted in our analysis. Let d_j ($j = 1, \ldots, p$) be the eigenvalues of spatial correlation matrix computed from n data sets, such that $d_1 > d_2 > \ldots > d_p$. A normalized statistic can be computed as $T_j = d_j / (\sum_{j=1}^{p} d_j)$. We now use a random number generator to generate independent sequences of length n for p independent Gaussian variables of zero mean and unit variance and compute the correlation matrix. The eigenvalues of the correlation matrix are then computed and the experiment is repeated, say, 100 times. If δ_j^k ($k = 1, \ldots, 100$) is the set of eigenvalues produced by the kth Monte Carlo experiment, the statistic analogous to T_j is $U_j^k = \delta_j^k / (\sum_{j=1}^{p} \delta_j^k)$. For fixed j, order the U_j^k so that $U_j^1 \le U_j^2 \le \ldots \le U_j^{100}$. If $T_j > U_j^{95}$ (U_j^{90} or U_j^{99}), then the jth eigenvalue is considered to be significant at the 95% (90% or 99%) level. The two statistics are estimated from a time series at each point on the grid and tested for their statistical significances.

3. Derivation of Global SST Modes

[10] The annually averaged SST time series of the global, Pacific, Atlantic, and Indian Oceans derived from the ERSST

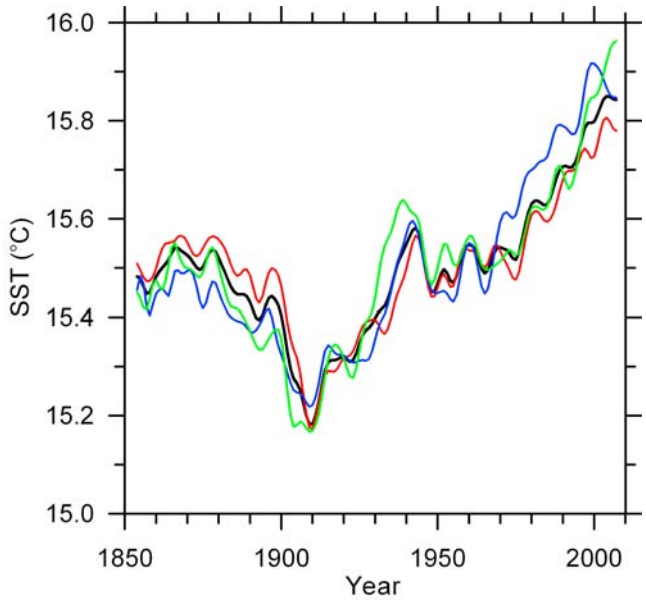

Figure 1. Annually averaged SST time series for the global (black), Pacific (red), Atlantic (green), and Indian (blue) oceans. The ERSST (Version 3) gridded monthly SSTs from January 1854 to December 2007 are used in the derivation. An offset for the three individual oceans with respect to the global mean (−0.041°C, 0.775°C, and −0.833°C for the Pacific, Atlantic, and Indian oceans, respectively) is removed in the plot to facilitate comparison.

gridded monthly product are plotted for the period 1854–2007 in Figure 1. As far as the global mean is concerned, the SST increases slightly around 1860 before decreasing gradually until about 1910 where a minimum is reached. After that an almost straightforward rise is seen during the following 100 years or so with only a short period of exception in the 1940s, suggesting that global warming is a basic trend in the past century. The SSTs of the three oceans largely resemble the global mean in their evolution. This is because the primary forcing of SST distribution (solar heating) has two geographical characteristics: Latitudinal dependency and longitudinal independency. Since the three ocean basins cover similar latitudes (except for the northern Indian Ocean) but different longitudes, the global and basin scale SST distributions are likely to share a zonal pattern with similar mean values, and are therefore coherent in their temporal variations. An interesting feature in Figure 1 is that the rate of SST rise appears to be the smallest for the Pacific, and the largest for the Indian Ocean (see their relative order before and after the turning point at about 1910). Also evident in Figure 1 is that the four curves fluctuate dramatically at timescales from interannual to interdecadal, a rich modality is expected to reside in the SST variability.

[11] The above argument is subsequently confirmed by the multipeak structure of Figure 2, in which the spatially averaged modal amplitudes of SST as a function of extracting period are shown. These amplitudes represent the energies associated with SST oscillations at a given periodicity as described in section 2. Each of the peaks in Figure 2 corresponds to a potential mode of SST variability. Those with amplitudes higher than the two neighboring peaks are defined as primary modes in this analysis, while the remaining ones are considered as secondary modes (note that a cutoff period is set to 80 years given the current span of data). The central periodicities of the identified global SST modes are given in Tables 1a and 1b, along with their order of peak values. For the seven primary modes (Table 1a), two fall into the interannual regime (modes B and C at 3.7 and 5.8 years) and four belong to the interdecadal regime (modes S, Q, I, and M at 9.0, 13.0, 21.2, and 62.2 years, they are so named to stand for the sub-, quasi-, inter-, and multidecadal modes which are consistent with their periodicity values), in addition to the dominant annual mode A. For the dozen of secondary modes (Table 1b), five are in the interannual regime (modes b–f at 2.7–7.6 years), and half of them are in the interdecadal regime (modes g–k and m at 10.0–33.5 years), plus the semiannual mode a. Altogether, we find seven separable modes in the so-called ENSO band, and ten in the IDO band, which cover a majority of the identified periodicities by previous investigators, suggesting that our analysis scheme

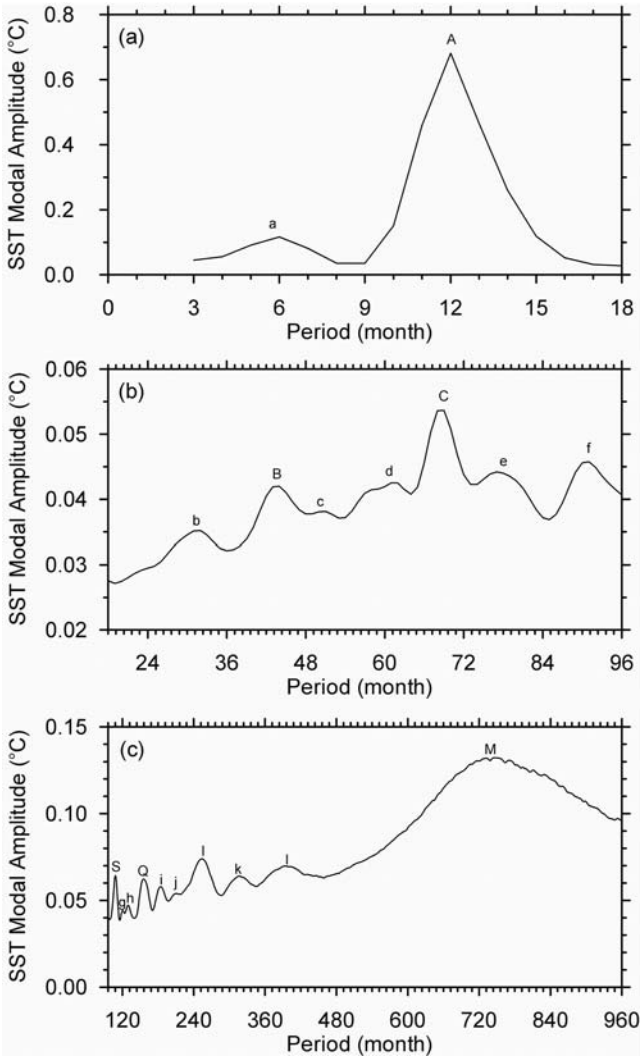

Figure 2. Globally averaged modal amplitude of SST as a function of extracting period for the (a) annual regime, (b) interannual regime, and (c) interdecadal regime. The identified peaks corresponding to primary modes are labeled with A, B, C, S, Q, I, and M, those corresponding to secondary modes are labeled with a–k and m.

Table 1a. Characteristics of Identified Primary SST Modes for the Global Ocean

Mode Index	Period for All Data[a] (Months)	Period for First Half[a] (Months)	Period for Second Half[a] (Months)	Order of Peak Values
A	12 (1.0)	12 (1.0)	12 (1.0)	1
B	44 (3.7)	45 (3.8)	43 (3.6)	7
C	69 (5.8)	71 (5.9)	68 (5.7)	6
S	108 (9.0)	106 (8.8)	108 (9.0)	4
Q	156 (13.0)	149 (12.4)	158 (13.2)	5
I	254 (21.2)	242 (20.2)	246 (20.5)	3
M	746 (62.2)	–	–	2

[a]Values given in parentheses are years.

is effective in efficient recovery of a modal spectrum. On the basis of the significance test scheme described in section 2, it is found that all primary modes, except for mode M, are highly significant at 0.01 level. Mode M and secondary modes a, b, e, f, i, k, and j are significant at 0.05 level. The remainders are largely at a lower significance level. It should be stressed that whether there are preferred IDO timescales is critical for several reasons, including the issue of dynamics and how understanding those dynamics should aid the development of an IDO monitoring and prediction system.

[12] There is a further interest to understand the stability or stationarity of the derived modes as a function of time. To do so, the 154 year SST record is split into two 77 year subdata sets, and their primary modes (except for mode M) are extracted and listed in Table 1a. It is found that all identified primary modes are present in the half-length record with a corresponding period drift of less than 5% compared to the full data set based estimate. A closer inspection shows that in the ENSO band (modes B and C), the primary modes shift toward a shorter period, while in the IDO band (modes S, Q, and I), the opposite is true. These results may have at least two implications: First, the identified primary modes are fairly stable and hence reasonably predictable. Second, assuming that the first half of the data record is dominated by natural variations, anthropogenic effect in the second period may tend to shorten the ENSO cycle, meanwhile prolong the IDO cycle. Such an argument is consistent with the fact that ENSO events occur more frequently after the 1970s [e.g., *Trenberth*, 1990]. In addition to frequency shift, it is also found that the derived amplitudes are mostly larger in the second period for the corresponding primary modes (not shown), providing further evidence to support the conclusion that the observed ocean warming may largely be because of the increase of anthropogenic gases in the Earth's atmosphere [*Levitus et al.*, 2001].

[13] We now examine the geographical expressions of the seven primary modes by plotting their modal amplitude on a global map (Figure 3). Mode A is the single most energetic mode (note the much larger color scale for Figure 3a), which dominates the seasonal cycle of the ocean. Figures 3b and 3c depict two typical ENSO modes which are collocated in space as a covarying westward extension zone in the equatorial Pacific with its origin in the Niño 1 + 2 region. In fact, *Chen and Li* [2008] observe that there are at least five ENSO-related SST submodes with well-defined periodicities during 1985–2003 (see their Figures 5e–5i). The frequency drift of ENSO may, however, prevent some of the short-lived submodes from being individually identified with a much longer data set. In addition to the primary ENSO zone in the equatorial Pacific, secondary highs also appear at midlatitudes of the two hemispheres, especially in the northern Pacific. S and Q are weak but significant primary modes at decadal timescales involving both tropical and extratropical oceans (see Figures 3d and 3e). They are found to be similar in their spatial patterns, both having an obvious ENSO-like signature in the equatorial ocean and a couple of modal maxima in midlatitude Pacific and Atlantic. They serve as a transition from an interannual to an interdecadal variability pattern. These two modes might be induced by the low-frequency fluctuation of ENSO [e.g., *Rodgers et al.*, 2004], but may also represent important ENSO-like decadal variability in the tropical oceans [e.g., *Zhang et al.*, 1997; *Luo and Yamagata*, 2001]. Mode I can be considered as a true start of the interdecadal regime with both annual and ENSO signals being largely suppressed (Figure 3f). Several zonally oriented regional highs are found at various latitudes of the three ocean basins with the one in the northern Atlantic being most significant. Mode M represents definitely the peak of IDV as far as SST is concerned (see Figure 2c). Its modal pattern is characterized by a clear Northern Hemisphere preference with two strong maxima in the northeastern Pacific and northwestern Atlantic (Figure 3g). This mode is so strong that its amplitude is more than twice that of the ENSO signals (compare Figures 2b and 2c). Such a pronounced oscillation with a repeating cycle of 62.2 years is certain to have a long-term impact on many aspects of nature and society. A new finding of potential importance is the apparent presence of multidecadal variability in the eastern tropical Pacific and Atlantic (Figure 3g), which was absent in previous analysis of shorter SST data sets [e.g., *Mestas-Nuñez and Miller*, 2006]. Note that the eastern tropical Atlantic signature appears to be stronger than its Pacific counterpart, providing additional evidence that the Pacific originated ENSO and the Atlantic leading IDO might be largely independent. It is argued that IDO, together with annual and El Niño oscillations serve as

Table 1b. Characteristics of Identified Secondary SST Modes for the Global Ocean

Mode Index	Period[a] (Months)	Order of Peak Values
a	6 (0.5)	1
b	32 (2.7)	12
c	51 (4.3)	11
d	61 (5.1)	9
e	77 (6.4)	10
f	91 (7.6)	8
g	120 (10.0)	6
h	130 (10.8)	7
i	185 (15.4)	4
j	209 (17.4)	5
k	316 (26.3)	3
m	402 (33.5)	2

[a]Values given in parentheses are years.

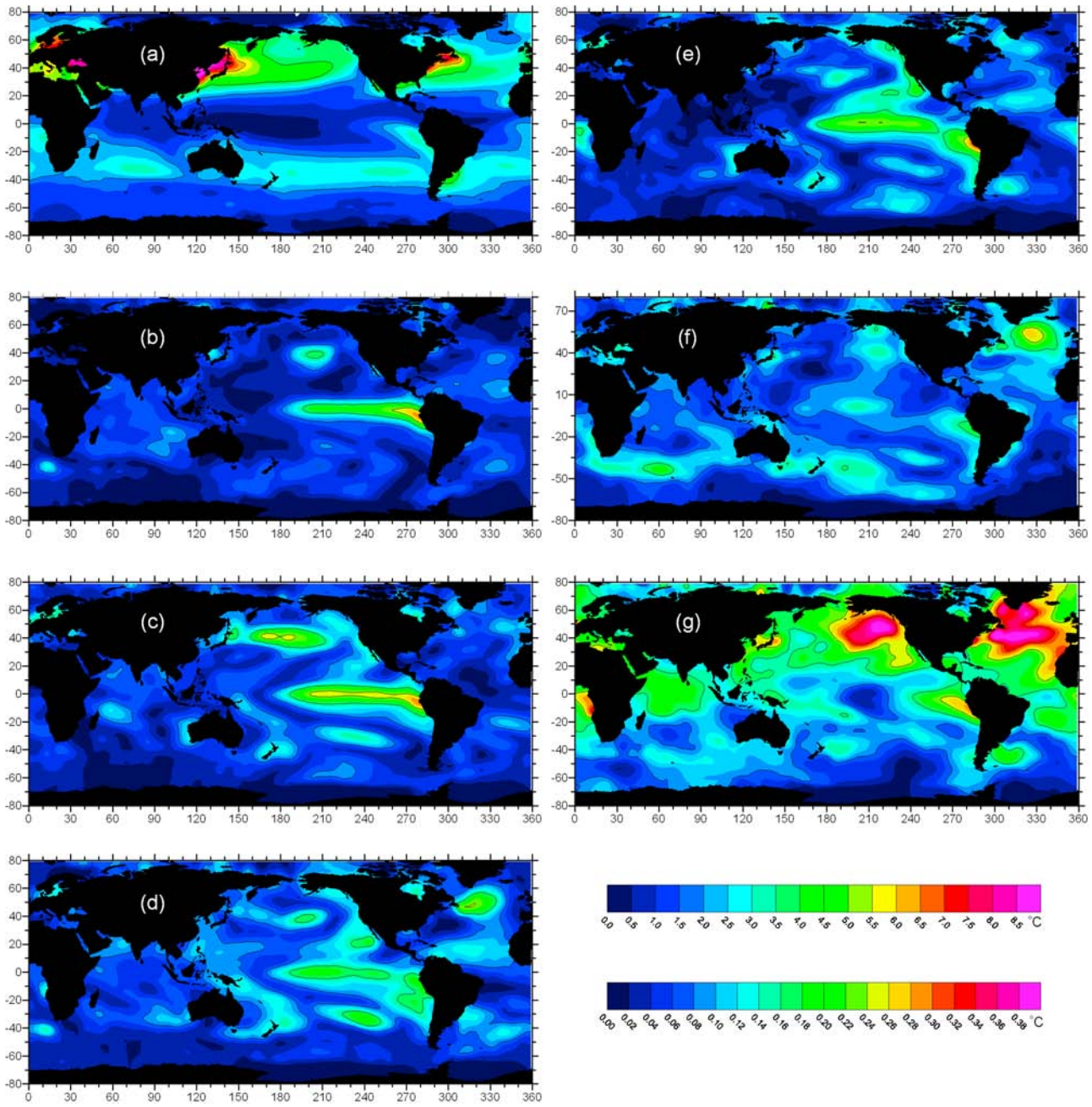

Figure 3. The spatial patterns of recovered SST amplitude at periods of the seven primary modes: (a) mode A, (b) mode B, (c) mode C, (d) mode S, (e) mode Q, (f) mode I, and (g) mode M. See Table 1a for their corresponding periodicities. The top color bar is for Figure 3a and the bottom one is for Figures 3b–3g.

an oceanic troika in affecting, if not driving, the long-term global climate change.

[14] Phase information of the seven primary modes is recovered along with amplitude following the procedures described in section 2, and is depicted at each grid point by the month of the period in which the maximum amplitude is reached. The obtained phase values are then normalized to a 12 month cycle to facilitate intercomparison. Finally, the normalized phase is binned into four quarters in order to capture major systematic oscillations, or the "seasons" of each mode. Figures 4a–4g show the phase distributions corresponding to the associated amplitudes in Figures 3a–3g.

[15] The annual phase pattern of SST shown in Figure 4a compares well with a map of its kind obtained in an earlier study [see Figure 2 of *Chen and Quartly*, 2005]. The lack of details in the present result is probably due to the much coarser resolution of the ERSST data set (5° versus 9 km). Focusing on the equatorial areas of the Pacific and Atlantic oceans, one finds that two annual amphidromes are clearly evident. ENSO-like patterns dominate modes B, C, S, and I in the areas of South Equatorial Current and Peru Current or the commonly referred Niño regions (Figures 4b–4e). These currents are basically driven by the southeast trade winds whose interannual and interdecadal variations might be a

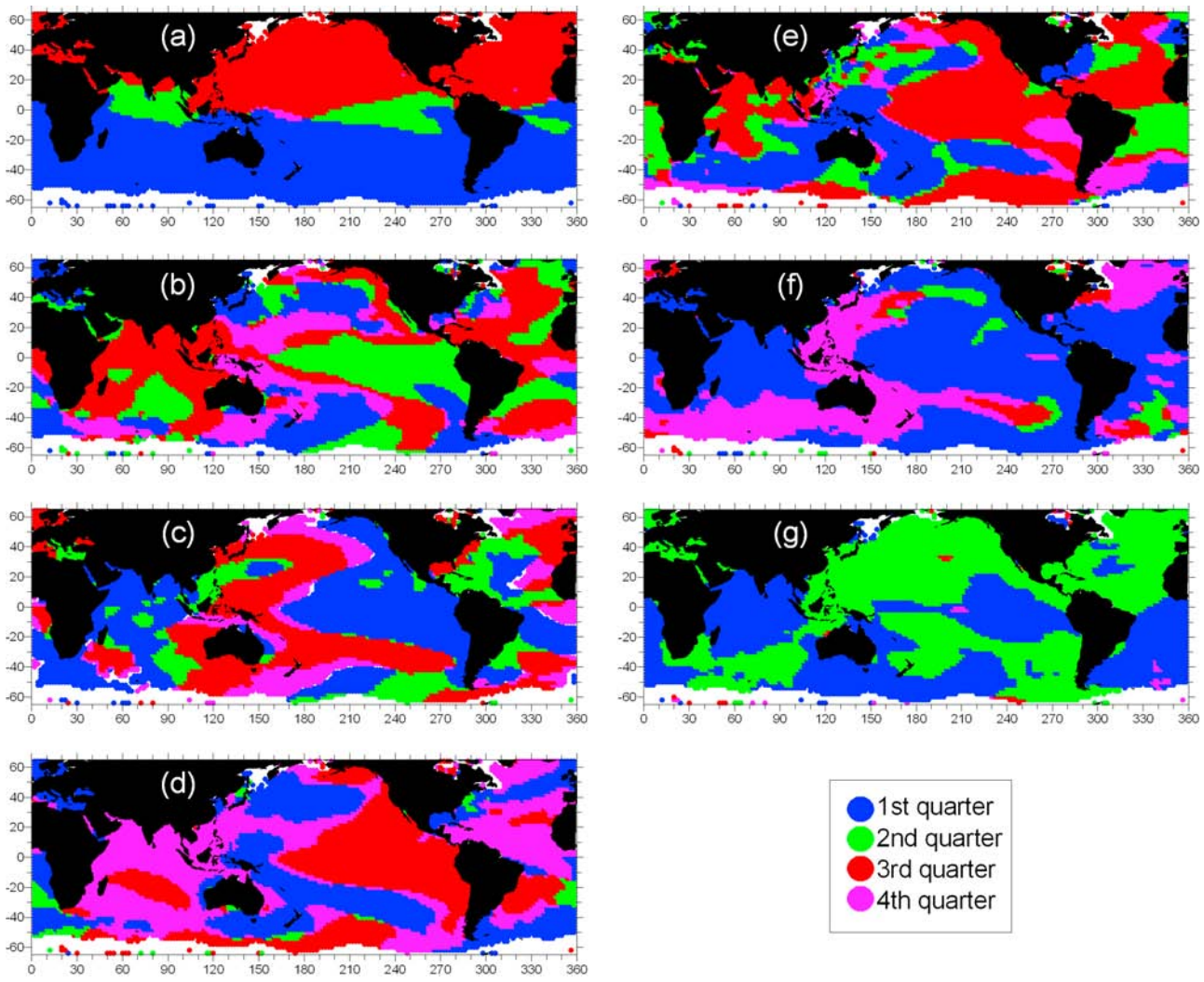

Figure 4. The spatial patterns of recovered SST phase at periods of the seven primary modes: (a) mode A, (b) mode B, (c) mode C, (d) mode S, (e) mode Q, (f) mode I, and (g) mode M. See Table 1a for their corresponding periodicities.

possible cause of the observed amplitude-phase coherence at corresponding modal frequencies. Signatures of the western boundary currents can be recognized as a systematic phase propagation in given modes, for instance, the Kuroshio and its extension in mode C (Figure 4c), and the Gulf Stream and its extension in mode B (Figure 4b). In contrast to Figures 4b–4e which are generally dominated by regional features, the phase structure of modes I and M is characterized by a two-season nature (Figures 3f and 3g), showing little correlation with their amplitude maxima (Figures 4f and 4g). This implies that the global oceans are rather consistent in their long-term variations with alternating multidecadal periods of warming and cooling.

4. Identification of Regional IDO Zones

[16] In this section, we would like to have an in-depth look into the spatiotemporal patterns of IDOs. Let us start by having an overview of the geographical distributions associated with the three general SST modal regimes. To do so, the period-dependant modal amplitudes are accumulated over the frequency band of each regime on point basis, resulting in three maps corresponding to the annual, ENSO, and IDO modal signals, respectively (Figures 5a–5c). Figure 5a is almost identical to Figure 3a, suggesting that the annual regime is absolutely dominated by the annual mode A. For the interannual regime, it comes with little surprise that the defining feature is located in the Niño regions along the central and eastern equatorial Pacific (Figure 5b). The counterparts of this major El Niño signal in the midlatitude North and South Pacific, as well as the "echoes" of the Pacific El Niño in the Atlantic and Indian oceans are also clearly displayed with well-defined signatures, implying that the impact of ENSO is truly global in both zonal and meridional dimensions.

[17] We now concentrate on the spatial pattern of the interdecadal modal regime (Figure 5c) which appears to be dramatically different from either the annual or the interannual regimes. The striking feature in Figure 5c is the two areas with maximum IDO energy in the northeastern Pacific and northwestern Atlantic, whose shapes resemble so much a pair of hoof prints of a horse. They are supposed to be the core

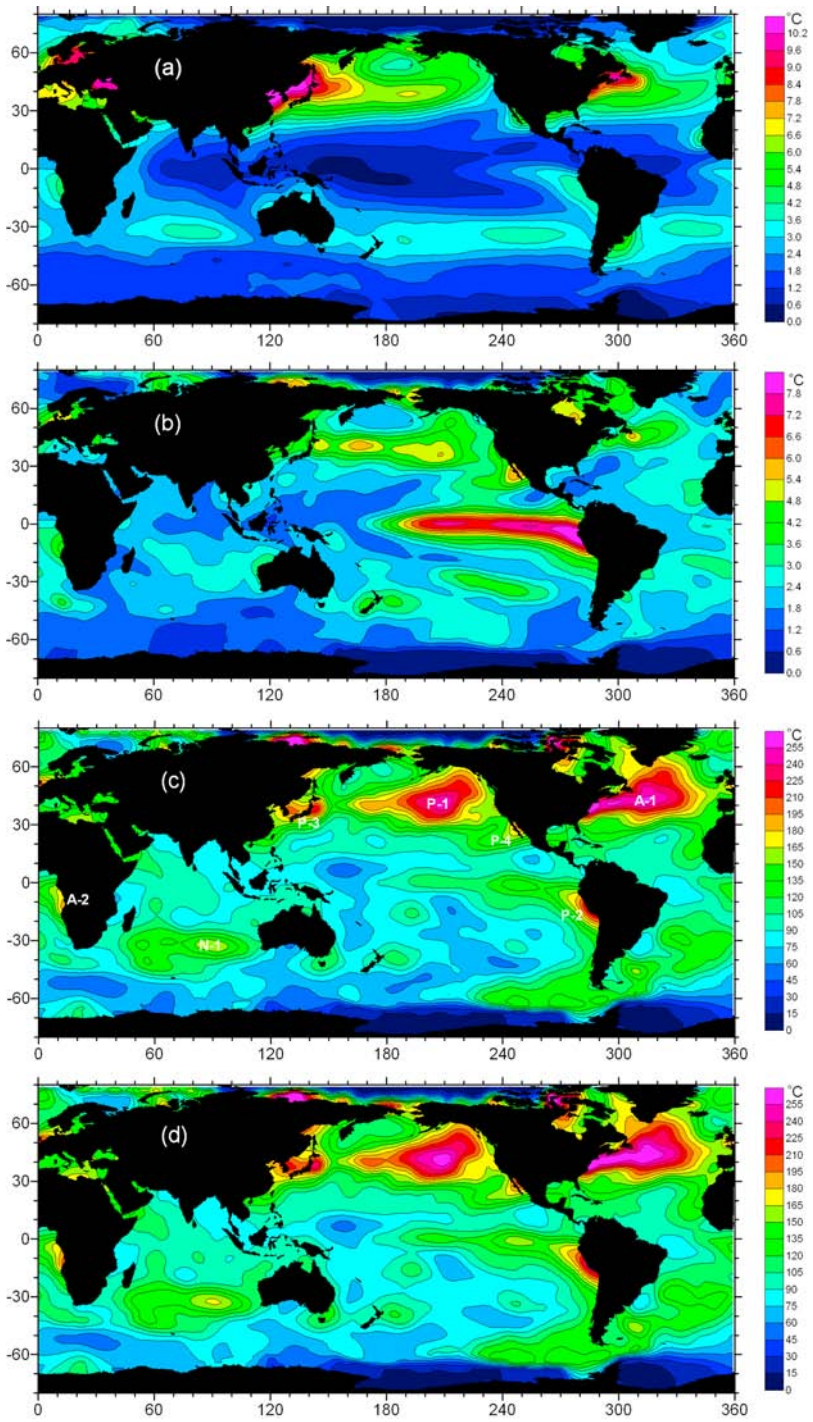

Figure 5. Geographical distributions of accumulated SST amplitude recovered for the three modal regimes and the total variability: (a) the annual regime, (b) the interannual regime, (c) the interdecadal regime, and (d) the total SST amplitude for all regimes.

regions of the intensively documented PDO and North Atlantic Oscillation (NAO) phenomena, which have been puzzling the scientists for at least two decades. These hoofprint-like zones are still mysterious because three basic questions related to PDO and NAO remain poorly understood: (1) What do they look like (characteristics)? (2) How do they behave (evolution)? (3) Why are they there (mechanism)? The present analysis, which is based on one of the best available up-to-date data sets, reveals that the two hearts of the IDO, commonly known as PDO and NAO (labeled as P-1 and A-1 in Figure 5c) are centered at (209°E, 41°N) and (314°E, 43°N) on a climatological basis. The size of the core zones of the two IDOs roughly equals the area of Australia ($\sim$768 km^2). We can also learn from Figure 5c that regions with significant IDOs are not only confined to P-1 and A-1. A couple of other areas with local SST modal maxima are also visible, as labeled with P-2–P-4 in the Pacific, with A-2 in the Atlantic, and with N-1 in the Indian Ocean. It is worth to

Table 2. Modal Characteristics of Major IDO Zones Identified With ERSST

Modal Zone[a]	Location	Central Period[b] (Months)			
		S	Q	I	M
PIDO-1	180°E–230°E, 30°N–60°N	107 (8.9)	142 (11.8)	217 (18.1)	779 (64.9)
PIDO-2	260°E–290°E, 0°–30°S	108 (9.0)	157 (13.1)	237 (19.8)	681 (56.8)
PIDO-3	120°E–160°E, 30°N–50°N	118 (9.8)	226 (18.8)	323 (26.9)	780 (65.0)
PIDO-4	230°E–260°E, 15°N–35°N	107 (8.9)	157 (13.1)	225 (18.8)	667 (55.6)
AIDO-1	280°E–340°E, 30°N–60°N	109 (9.1)	156 (13.0)	262 (21.8)	798 (66.5)
AIDO-2	350°E–20°E, 0°–30°S	120 (10.0)	150 (12.5)	269 (22.4)	719 (59.9)
NIDO-1	40°E–110°E, 20°S–50°S	107 (8.9)	163 (13.6)	255 (21.3)	612 (51.0)

[a]These zones are abbreviated as P-1–N-1 in Figures 5 and 7 as well as in the text for simplicity.
[b]Values given in parentheses are years.

mention that basin-based naming for the IDOs zones may sometimes lead to confusion in a geographical sense. For example, the term PDO may have several aliases [*Mantua and Hare*, 2002], such as Interdecadal Pacific Oscillation [IPO, *Power et al.*, 1999] and North Pacific Oscillation [NPO, *Gershunov and Barnett*, 1998]. Since the IDOs appear to be geographically dependent, we propose to use unified regional names, analogous to the Niño regions, to specify the above zones. As such, PDO is formally referred to as PIDO-1, but is abbreviated as P-1. The names and ranges of the seven IDO zones are defined in Table 2 for further individual analysis (note that we use "N" instead of "I" for the Indian Ocean to avoid possible confusion with mode I). To further validate the proposed scheme, the accumulated total variability amplitude for all modal regimes is also plotted in Figure 5d. Not surprisingly, the total accumulation of modal amplitude basically resembles the interdecadal regime because of the much broader width of its spectrum. The manifestation of the annual and ENSO signals are both discernible but are comparatively weak as a result of their narrow peaks.

[18] As far as the Pacific and Atlantic oceans are concerned and to some extent for the Indian Ocean, a comparison between Figures 5b and 5c leads to a general conclusion that ENSO signals exceed the IDOs and dominate the variability of the tropical oceans, while the opposite is true for the extratropical oceans. A further inference which can be made is that the ENSO/IDO interaction might be rather weak if exists. In fact, these arguments are not new for the Pacific Ocean. *Zhang et al.* [1998] observe an interdecadal standing SST mode with opposite signs in the North and tropical Pacific. They find that the interdecadal mode explains more variance in the North Pacific than in the Tropics, whereas the interannual modes contribute more to the total variance in the Tropics. They further point out that the interdecadal and the interannual modes might be of different geographical and possibly of different physical origins. Recently, *Mestas-Nuñez and Miller* [2006] also show a more extratropical preference for the interdecadal Pacific variability using rotated EOF analysis, where the original definition of the PDO mixes up ENSO with interdecadal variability. Our findings not only confirm these results in the Pacific, but also extend them to the Atlantic and even to the Indian Ocean.

[19] The IDO behaviors in the modal active zones identified in Figure 5 are further examined by plotting their individual SST amplitude as a function of period (Figure 6). Apparently, the four primary IDO modes (S, Q, I, and M) are all confirmed in the seven zones with little ambiguity, suggesting that a canonical pattern with four leading IDO

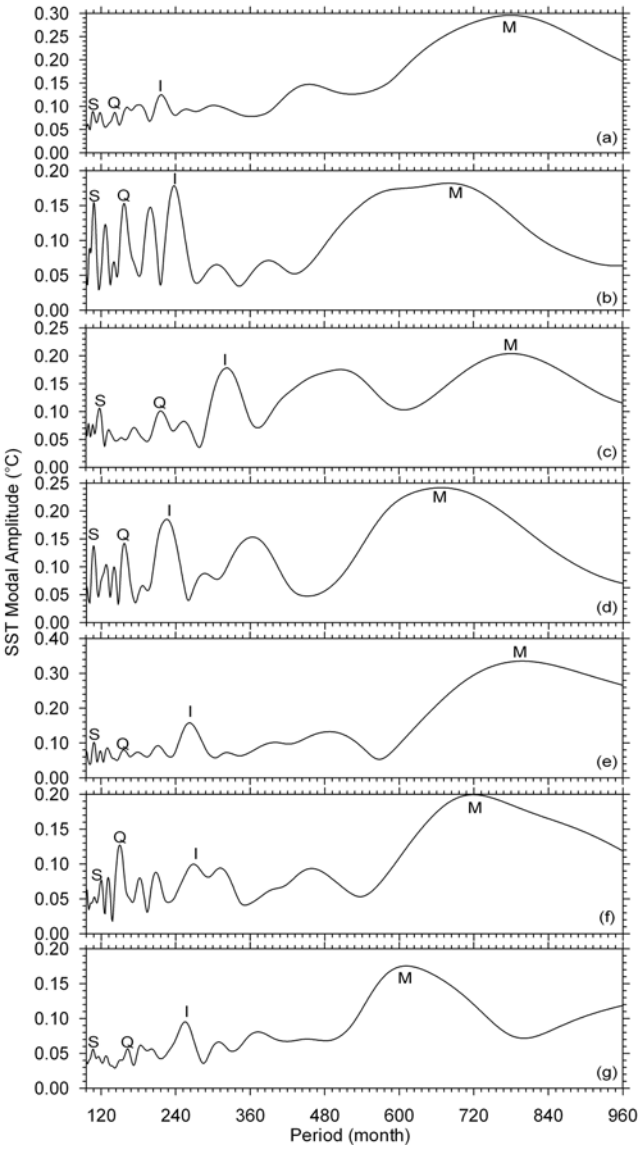

Figure 6. Spatially averaged modal amplitude of SST as a function extracting period for the seven IDO active zones: (a) P-1, (b) P-2, (c) P-3, (d) P-4, (e) A-1, (f) A-2, and (g) N-1. The identified peaks corresponding to the primary IDO modes are labeled with S, Q, I, and M, respectively.

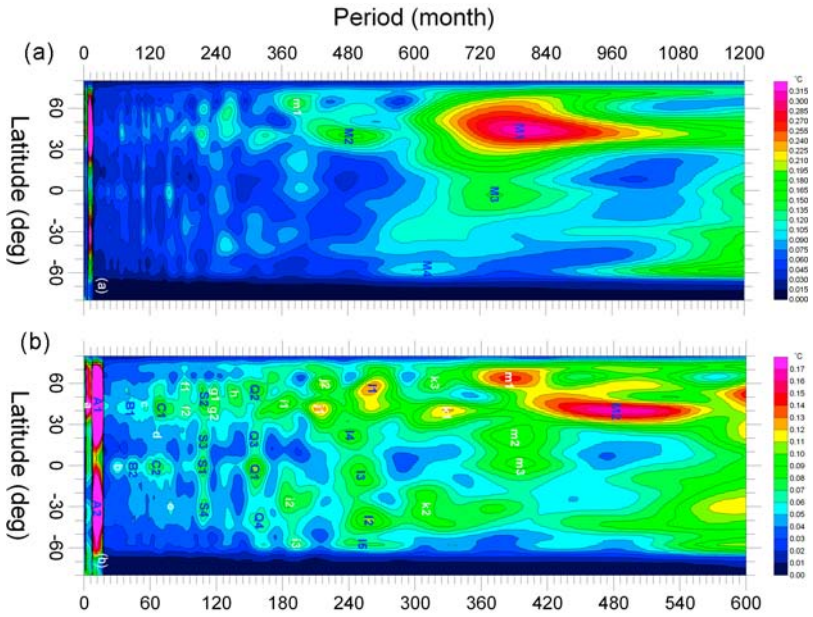

Figure 7. (a) Period-latitude diagram of modal amplitude derived from ERSST data. (b) An enlargement of Figure 7a for the high-frequency part. Both diagrams are mean maps averaged over all longitudes. The primary submodes are indicated in blue, while the secondary ones in white.

modes is geographically robust. Recent model experiments also suggest that PDV is composed of two distinct modes: A decadal to bidecadal tropical Pacific mode and a multidecadal North Pacific mode. [e.g., *Wu et al.*, 2003]. But the coexisting nature of the two identified IDO modes is not clarified. Regional frequency shifts of these modes, however, are also evident. The maximum periodicity difference (excluding P-3) is found to be 1.1, 2.8, 4.3, and 15.5 years for modes S, Q, I, and M, respectively (see Figure 6 and Table 2). The modes Q and I of P-3 are considerably apart from other IDO active zones, possibly as a result of the inclusion and interaction of the semienclosed Japan Sea and eastern China Seas where the hydrological situation is much more complex compared to the open ocean, and the main body of the Kuroshio current where well-known mesoscale eddy dynamics is prevalent [e.g., *Ichikawa and Beardsley*, 2002]. Note that, in addition to the general consistency, each of the selected zones appears to have half a dozen or so of secondary IDO modes as indicated in Table 1b, confirming the diversity and regionality of individual modal pattern.

5. Fine Spatiotemporal Patterns

[20] The fine patterns of the identified SST modes can be further revealed by making a plot of latitude as a function of extracting period (Figure 7). Keep in mind that a vertical structure in Figure 7 corresponds to a sharp peak while a horizontal one corresponds to a flat high in the diagram. It can be seen that roughly below 400 months, the contours are dominated by narrow peaks associated with relatively low energy, except for the annual and semiannual frequencies where the most energetic peaks are found. In contrast, signals with a period longer than about 400 months are much stronger but less sharper. Such characteristics imply that, statistically, annual cycle is most easily predictable, followed by ENSO cycle which is now predictable on the order of 1–2 years in advance [*Luo et al.*, 2008]. Unfortunately, the inter- or multidecadal oscillations are most unpredictable given their much broadened spectrum features.

[21] What also becomes immediately apparent is that all of the primary modes and most of the secondary modes have more than one origins with a wide coverage of latitude (see the modal labels in Figure 7). The equatorial regions and the midlatitude areas of the two hemispheres are three mode-rich belts in the global ocean. Surprisingly, a rather systematic north-south symmetry across the equator exists for the timescales ranging from annual to approximately 360 months (or ~30 years, see Figure 7b). This confirms a similar finding with a Pacific IDO at timescales of 15–20 years by *Chao et al.* [2000]. Our results indicate that such a symmetric feature is not limited to a specific interdecadal band, nor is it unique to the Pacific Ocean.

[22] We concentrate again on the primary modes and start from the interannual regime (the annual mode A is so distinct and well documented that it deserves little further discussion). The realizations of modes B and C both appear in pair, with one near the equator and the other around 40°N (Figure 7b). Each of them is basically restricted to a 20° meridional band with limited zonal impact, which is appropriate to be recognized as a regional mode. In the interdecadal regime, modes S, Q, and I are all characterized by a series of well-defined modal maximum, meaning that each primary mode is in fact composed of a number of independent submodes with slight frequency shifts. The uncertainty in periodicity is within ±2 months for the sub- and quasidecadal modes (S and Q). For the interdecadal mode I, however, the period of the five identified submodes varies from 241 months with I4 to 261 months with I1, having a medium value of 254 months. It is also found that these submodes are somehow regularly distributed with respect to latitude (see S1–S4, Q1–Q4, and I1–I5 in Figure 7b). Interestingly, it is further observed that both the latitudinal coverage and the

associated energy of the submodes increase generally with modal period for B, C, S, Q, and I, implying that lower frequency oscillations are more likely to have a stronger global impact in terms of scale and intensity. This argument is immediately supported by examining mode M in Figure 7a. This mode, which consists of at least four submodes with a period of 488–803 months, is perhaps the longest oscillation that can be identified with fair confidence given the maximum length (1848 months) of the present data set. Unlike other primary modes discussed above, mode M has a clear geographical preference to the Northern Hemisphere with considerable frequency dispersion. The single dominant submode (M1) favors 30°–60°N, and the other three submodes (M2–M4) center around 40°N, 5°S, and 55°S, respectively. It should be emphasized that, given its remarkably large-scale and high-concentration of modal energy compared to the leading interannual modes (e.g., B1,2 and C1,2), mode M1 can be considered as the most powerful engine in driving the long-term global climate change. The huge potential impact of IDO in general and M1 in particular is in no way less important than ENSO. In fact, the importance of M1 and the recognition of its climatic effects have been and are being experienced. Examples of its consequences are evidenced in variability of Atlantic hurricane activity [e.g., *Goldenberg et al.*, 2001], and of rainfall over North America [e.g., *Enfield et al.*, 2001]. These papers have been cited a lot, indicating the emerging interests in this topic.

[23] A joint view of Figures 5 and 7 leads to the judgment that, on the one hand, a couple of primary and secondary modes ranging from intra-annual to multidecadal may coexist in each of the identified modally active zones. On the other hand, any of the major modes may be found at several locations with a wide range of longitude and latitude in more than one of the ocean basins. The IDO characteristics of multimodality (for a given region) and multiregionality (for a given mode), however, have never been fully clarified in previous investigations.

6. Comparisons and Discussions

[24] At this point, we would like to introduce a comparison between our results and those published in the literature. Using several independent instrumental data sets including SST and sea level pressure (SLP), *Minobe* [1997] discovers a 50–70 year climate variability over the North Pacific and North America, which coincides with a 60 year oscillation in the populations of sardine and anchovy in the eastern North Pacific. Our mode M with a periodicity of 51.0–66.5 years (Table 2) provides an excellent confirmation of the above finding and implies that the identification and understanding of this multidecadal mode will have important long-term socio-economic effects. The existence of a regular period of 12–14 years in the North Atlantic SST is observed by *Sutton and Allen* [1997], which appears to be in good agreement with our 13 year mode Q for the A-1 zone (Table 2). *Moron et al.* [1998] report that near-decadal oscillations exist primarily over the North Atlantic, but also over the South Atlantic and the Indian Ocean, which are consistent with the identified IDO zones of A-1, A-2, and N-1 (see Figure 5c). Their results indicate a 13–15 year oscillation with a seesaw pattern between the Gulf Stream region and the North Atlantic Drift, which is generally consistent with our 12.5–13.6 year quasidecadal mode Q for these regions (see Table 2). In a work by *Enfield and Mestas-Nuñez* [1999], three non-ENSO low-frequency modes are characterized. The first mode corresponds to the Pacific interdecadal variability whose spatial pattern is similar to PDO and coincides well with the areas covered by P-1, P-2, and P-4 zones (see Figure 5c). It is believed that the first mode they identified with a period of 10–20 years actually consists of at least six quasidecadal and interdecadal modes in the above zones with a central period varying from 11.8 to 19.8 years (see Table 2). Their second mode corresponds to the Pacific multidecadal variability with highest loadings extending westward from 160°W along 45°N. This multidecadal mode is basically our mode M of the P-1 zone with a period of 64.9 years (see Figure 5c and Table 2). Their third mode corresponds to the Atlantic multidecadal (15–40 years as described) variability which is most evident in the high latitudes of the North Atlantic, immediately south of Greenland. This agrees very well with the A-1 zone in space, whereas our result suggests two interdecadal periods at 21.8 and 66.5 years, respectively. In an accompanying study, *Mestas-Nuñez and Enfield* [1999] derive six-localized non-ENSO modes: The North Atlantic multidecadal mode, the eastern North Pacific interdecadal mode, the eastern tropical Pacific interdecadal mode, the central tropical Pacific interdecadal mode, the North Pacific multidecadal mode, and the South Atlantic interannual-to-interdecadal mode. Apparently, most of these leading modes fall into the mode-active zones on our map (compare their Figures 1–6 with our Figure 5c). In fact, what they have reported might be a portion of IDO modes that exist in those regions (see Table 2). They conclude that non-ENSO SST variability is more regional than global in nature. This view is shared by *Mizoguchi et al.* [1999] who also find three multi- and quasidecadal variations of SST in the North Atlantic. They describe their mode 1 as a very slow oscillation with an approximate 42 year period, having basin-wide spatial evolution. Their modes 2 and 3 are a quasidecadal fluctuation with periods of 14.4 and 13.9 years, propagating from the Labrador Sea eastward following the North Atlantic Current and the subpolar gyre. Although the three quasi- and multidecadal modes in the North Atlantic are confirmed in our zone A-1, the central periods estimated in this analysis are 13.0, 21.8, and 66.5 years (corresponding to modes, Q, I, and M, see Table 2), respectively. The reason for such a considerable discrepancy could basically be attributable to the fact that the lengths of data sets used in the two studies are somewhat incomparable: 154 years versus 46 years. In fact, one has to be very cautious in interpreting a 42 year signal derived from a 46 year data set. Similar cautions have to be applied with the 70 year Pacific multidecadal mode as tentatively identified by *Chao et al.* [2000] using a 92 year SST time series. Mode M here with an average period of 62.2 years could be an improved estimate of the same oscillation.

[25] More recently, *Tourre et al.* [2001] reveal coherent patterns of low-frequency 20th century Pacific SST and SLP variations from 30°S to 60°N, in which a decadal mode peaking at 9–12 year periods, and an interdecadal mode peaking at 12–25 year periods are identified. These are likely to be the combined manifestations of our modes S, Q, and I in periodicity, and our zones P-1, P-2, and P-4 in location. The

investigation by *Mestas-Nuñez and Enfield* [2001] is focused on the Niño-3 region (5°S–5°N, 210°E–270°E) where they find the residual non-ENSO low-frequency SST variability is concurrently correlated with a mode associated with an interdecadal modulation of ENSO, and another mode associated, in their words, with interdecadal aspects of the PDO. This confirms the argument that multimodality is a common feature for the major oscillation zones. In contrast, *Lohmann and Latif* [2005] observed a decadal mode with a period of about 10 years in SST of the central western Pacific. Note that they choose the Niño-4 region (5°S–5°N, 160°E–210°E) to perform their analysis on the basis of previous observations which indicate that the decadal SST variability is particularly strong in the western central equatorial Pacific [e.g., *Trenberth and Hurrell*, 1994]. Our results suggest, however, the Niño-4 region is not among the most dynamic zones as far as the IDO modes are concerned, although it is on the tip of the prominent ENSO tongue (see Figures 5b and 5c). This confirms, from another perspective, that quasidecadal or interdecadal mode is not an exclusive characteristic for particular regions. *Luo and Yamagata* [2002] are among the few who explicitly identify a local mode in the P-3 zone with a period of about 10 years (see their Figure 2d) which coincides well with that of our mode S (9.8 years). The P-3 zone is often missing is previous studies probably because its contribution to the variance over the entire domain is relatively weak (note that it is the fifth SVD mode by *Luo and Yamagata* [2002]). A joint frequency domain analysis of SST and SLP anomalies over the global ocean is performed by *White and Tourre* [2003] who find a quasidecadal (~11 year period) and an interdecadal (~17 year period) wave. On each period scale, the global traveling wave is composed of zonal wave numbers −1 and −2, directed eastward with a phase speed that takes 1–2 cycles to traverse the global ocean between 40°S and 20°N. Their results are in qualitative agreement with ours in both period and space. *Frauenfeld et al.* [2005] uncover a distinctly interdecadal signal at timescales longer than 20 years originated from the climate of the tropical Pacific, which they call interdecadal Pacific signal (IPS), by examining the coupled behavior of SST and Northern Hemisphere atmospheric circulation. They argue that the IPS is likely a component of the PDO, and vice versa. This can be understood as such that the IPS- and PDO-dominated regions may contain similar submodes in their interdecadal variabilities, which is exactly the case revealed by our analysis (Table 2). A fascinating recent study by *McKinnell and Crawford* [2007] indicates that temperature variability in the northeastern Pacific, even some of those currently attributed to ENSO, are influenced by the 18.6 year lunar nodal cycle. This might be one of the reasons that explain the downward shift of the central periodicities of mode I for the P-1 and P-4 zones compared to other modal regions from a global mean of 21.2 years to 18.1 and 18.8 years, respectively.

[26] Very recently, *Guan and Nigam* [2008] point out that PDV is characterized by two modes: The Pan-Pacific mode which has a horseshoe structure with the closed end skirting the North American coast, and a quiescent eastern equatorial Pacific. The mode exhibits surprising connections to the tropical/subtropical Atlantic, with correlations there resembling the Atlantic multidecadal oscillation. The second decadal mode, the North Pacific mode, captures the 1976/1977 climate shift and is closer to the PDO. They emphasize the striking links of the North Pacific mode to the western tropical Pacific and Indian Ocean SSTs, which can be generalized as a kind of zonal and meridional regularity of the submodal regions. It should be added that proxy environmental records such as tree ring and Pacific coral-based climate reconstructions tracing back to at least 1600 also suggest that PDO variations with a 23 year regime shift and a 50–70 peak periodicity are evident [*Mantua and Hare*, 2002], and hence are in general consistent with instrumental records, especially with our modes I and M (Table 1a).

[27] Physical explanation on the mechanism of the decadal-to-multidecadal oscillations in SST as well as in the global climate system remains a controversial issue at present time, and will be a challenging task in the future. As far as the decadal-to-interdecadal modes in the tropical oceans are concerned, a number of mechanisms have been proposed which include tropical-extratropical air-sea interactions, impacts from extratropical low-frequency variations, intrinsic tropical processes, stochastic atmospheric forcing, nonlinear processes within the climate system, and so on [e.g., *Mantua and Hare*, 2002; *Luo et al.*, 2003; *Cibot et al.*, 2005; *Montecinos and Pizarro*, 2005]. As for the possible causes of the multidecadal modes of SST in the midlatitude oceans, proposed hypotheses can be classified into two categories: External oscillatory forcing such as variations in solar radiation, and internal oscillation of the ocean-atmosphere system [e.g., *Minobe*, 1997; *Latif*, 2006].

[28] On the basis of the obtained results of the periodicity, amplitude, and phase of the major SST modes, as well as their spatial distribution and temporal variation, our hypothesis on the origin and generation of these principal oscillations is that they are primarily controlled by local/regional forcing, meanwhile significantly modulated by teleconnected remote dynamics. The spatiotemporal patterns of these oscillations are basically determined by natural forces, but can be considerably modified by anthropogenic impacts. An exemplary scenario of the formation of modes S and Q in the P-2 and A-2 zones (Figure 5) might be understood as such: Remotely forced by the tropical warm (cold) SST anomaly in the eastern equatorial Pacific/Atlantic, a southeast-northwest oriented negative (positive) wind stress curl is excited in the southwest of the tropical Pacific/Atlantic. This causes the thermocline to shoal as a result of Ekman transportation, giving rise to negative (positive) subsurface temperature anomalies. These anomalies then move northwestward to the western central equatorial Pacific/Atlantic, turn eastward and propagate along the equator to reverse the process in the eastern Pacific/Atlantic. In contrast, the multidecadal modes I and M in the P-1 and A-1 zones can be plausibly explained by the dynamical oceanic response to stochastic wind stress forcing as internal to the North Pacific/North Atlantic, since their variabilities evolve largely independent of the variations in the tropical Pacific/Atlantic [see *Latif*, 2006]. Accordingly, ocean spectra such as SST spectra are red up to multidecadal time scales, while atmospheric spectra are basically white.

7. Summary and Conclusions

[29] Study of ENSO and its impact on global climate change has been a very popular subject of oceanographic and atmospheric sciences in late 1900s. Turning to the 21st

century, it certainly has at least one more competitor, IDO. Interestingly, the classic descriptions of the two phenomena are both linked with fishery. The term El Niño (the oceanic component of ENSO) was originally used by fishermen along the coasts of Ecuador and Peru to refer to a warm ocean current that typically appears around Christmas time and lasts for several months, during which fish are less abundant [*Philander*, 1990]. These exceptionally strong warm waters not only disrupt the normal lives of the fishermen, but also bring dramatic changes in climate. A few decades later, fisheries scientist Steven Hare coined the term "Pacific decadal oscillation" (a special class of IDO) in 1996 while researching connections between Alaska salmon production cycles and Pacific climate [*Mantua et al.*, 1997]. PDO has ever since been described as a long-lived El Niño-like pattern of Pacific climate variability. Therefore, ENSO and PDO (or IDO in general) are "twin episodes" in both nature and science.

[30] Being twin episodes, ENSO and PDO (IDO) must have a number of similarities and connections: Both are multimoded with indices defined with SST, both have collocated and geometrically confusable signatures in the tropical and midlatitude Pacific, both have profound impacts on marine and terrestrial ecosystems as well as global and regional climate, and so forth. In spite of these similarities, their differences are fundamental. First, accumulating evidence suggests that IDO and ENSO are probably of independent origins [e.g., *Latif*, 2006]. Second, the general lifetime (periodicity) of IDO is roughly an order of magnitude longer than ENSO ($\sim$50 years versus $\sim$5 years). Third, the global intensity of IDO could be twice as much as ENSO (see Figures 5b and 5c). Fourth, the most energetic IDO zone is found in the extratropical North Atlantic (the A-1 zone in Figure 5c), whereas that of ENSO is well known to be the eastern equatorial Pacific (the Niño regions). Moreover, the significantly affected area of IDO is much larger than that of ENSO in terms of zonal and meridional coverage (Figure 7).

[31] In this study, a detailed analysis aimed at revealing the basic patterns of oceanic IDOs with fine structures is carried out using a reconstructed monthly SST data set from 1854 to 2007, along with an optimized modal extraction strategy, yielding the following main results and conclusions.

7.1. Data

[32] Most of the previous researches on IDV have been based on the period of record from 1950 onward (see Table 2 of *Chen and Li* [2008]), in which the reverse of SST trend around 1909 (see Figure 1) is absent. This makes a substantial difference in terms of multidecadal oscillation. Even with a 94 year record spanning 1900–1993, *Zhang et al.* [1997] are not convinced that a formal modal separation involving interdecadal variability is meaningful. On the basis of the results presented in this analysis, however, it can be concluded that present length of 154 years of observational data allows the principal modes of IDV to be identified with reasonable confidence.

7.2. Methodology

[33] It is argued that since classic EOFs are designed to efficiently describe global variance of the data, they generally do not represent a large fraction of the variance, and hence do not necessarily identify intrinsic modes of climate variability, in a particular region [e.g., *Vimont*, 2005]. The rotated EOF approach is expected to overcome part of the difficulties, as used by *Mestas-Nuñez and Enfield* [1999] in which most of the key regions for interdecadal variability are identified. The two-dimensional propagating modal extraction technique adopted in this analysis provides another alternative which has the advantage of being space-time decoupled and fully data adaptive, and appears to be more effective and efficient compared to many of the commonly used methodologies in retrieving intrinsic components from a complex modal system.

7.3. Results

[34] Among the dozens of potential IDO modes in global SST variability (some have been identified by previous investigators during the past two decades), four of them are, in many aspects, critical: The subdecadal mode at 9.0 years, the quasidecadal mode at 13.0 years, the interdecadal mode at 21.2 years, and the multidecadal mode at 62.2 years. The combination of these high-profile modes forms a canonical expression of IDV in the frequency domain. In the space domain, seven modally dynamic zones, analogous to the four Niño regions with ENSO, are clearly identified: P-1 to P-4 in the Pacific, A-1 and A-2 in the Atlantic, and N-1 in the Indian Ocean. The distinct signatures of IDO are most visible in the extratropical oceans, especially in the North Atlantic/North Pacific sectors (see A-1 and P-1 in Figure 5c), and secondary signatures exist in the tropical areas (see P-2 and A-2 in Figure 5c), while the opposite is true for ENSO. However, IDO-dominated regions do not prevent major ENSO modes from coexistence, and vice versa. Furthermore, it is recognized that although some of the distinct modes appear in a geographically correlated way, they are usually out of phase in the time domain (see Figure 4). Nevertheless, the array of primary modes with respect to their major active zones yields a sophisticated yet canonical pattern of ENSO/IDO, leading to a basic conclusion that multimodality (for a given region) and multiregionality (for a given mode) are fundamental features of the ENSO/IDO system. Accumulating evidence also suggests that the IDO modes are naturally and internally generated, but with significant modulations/modifications by external and anthropogenic forces. Further understanding of their mechanisms will have to rely on progress in both observational and theoretical studies.

[35] IDO science is relatively new compared to ENSO science, but insights into the IDOs catch up with an accelerating pace since the last decade of the 20th century. Benefiting from the unique advantage of a two-dimensional propagating mode extraction technique and an up-to-date SST data set, the results presented in this paper are so far, to our knowledge, the most detailed and complete ones of their kind in characterizing IDO-related modal properties and revealing their spatiotemporal patterns. This argument is supported by the fact that numerous previous findings of similar nature can retrieve their "footprints" in our unified framework. Precise and systematic identification of these intrinsic modes is very important, since understanding of quasiperiodic oscillations in natural variability can significantly increase the predictability of the ocean-atmosphere system and improve confidence in the detection of anthropogenic climate change. Hopefully, the results and conclu-

sions of this study will lead to better-targeted research efforts into underlying dynamics and make a significant contribution to the emerging IDO science in the future.

[36] **Acknowledgments.** This research was jointly supported by the Natural Science Foundation of China under Projects 40730530 and 40675016, the National Basic Research Program of China under Project 2009CB723903, and the National High-Tech Research and Development Program of China under Project 2008AA121701. The two anonymous reviewers are greatly appreciated for their helpful comments and constructive suggestions on an earlier version of this paper.

References

Chao, Y., G. M. Ghil, and J. C. McWilliams (2000), Pacific interdecadal variability in this century's sea surface temperatures, *Geophys. Res. Lett.*, *27*, 2261–2264, doi:10.1029/1999GL011324.

Chen, G. (2006), A novel scheme for identifying principal modes in geophysical variability with application to global precipitation, *J. Geophys. Res.*, *111*, D11103, doi:10.1029/2005JD006233.

Chen, G., and H. Li (2008), Fine pattern of natural modes in sea surface temperature variability: 1985–2003, *J. Phys. Oceanogr.*, *38*, 314–336, doi:10.1175/2007JPO3592.1.

Chen, G., and G. D. Quartly (2005), Annual amphidrome: A common feature in the ocean?, *IEEE Geosci. Remote Sens. Lett.*, *2*, 423–427, doi:10.1109/LGRS.2005.854205.

Cibot, C., E. Maisonnave, L. Terray, and B. Dewitte (2005), Mechanisms of tropical Pacific interannual-to-decadal variability in the ARPEGE/ORCA global coupled model, *Clim. Dym.*, *24*, 823–842, doi:10.1007/s00382-004-0513-y.

Enfield, D. B., and A. M. Mestas-Nuñez (1999), Multiscale variabilities in global sea surface temperatures and their relationship with tropospheric climate patterns, *J. Clim.*, *12*, 2719–2733, doi:10.1175/1520-0442(1999)012<2719:MVIGSS>2.0.CO;2.

Enfield, D. B., A. M. Mestas-Nunez, and P. J. Trimble (2001), The Atlantic multidecadal oscillation and its relationship to rainfall and river flows in the continental U.S., *Geophys. Res. Lett.*, *28*, 2077–2080, doi:10.1029/2000GL012745.

Frauenfeld, O. W., R. E. Davis, and M. E. Mann (2005), A distinctly interdecadal signal of Pacific ocean-atmosphere interaction, *J. Clim.*, *18*, 1709–1718, doi:10.1175/JCLI3367.1.

Gershunov, A., and T. P. Barnett (1998), Interdecadal modulation of ENSO teleconnections, *Bull. Am. Meteorol. Soc.*, *79*, 2715–2726, doi:10.1175/1520-0477(1998)079<2715:IMOET>2.0.CO;2.

Goldenberg, S. B., C. W. Landsea, A. M. Mestas-Nuñez, and W. M. Gray (2001), The recent increase in Atlantic hurricane activity: Causes and implications, *Science*, *293*, 474–479, doi:10.1126/science.1060040.

Guan, B., and S. Nigam (2008), Pacific sea surface temperatures in the twentieth century: An evolution-centric analysis of variability and trend, *J. Clim.*, *21*, 2790–2809, doi:10.1175/2007JCLI2076.1.

Ichikawa, H., and R. C. Beardsley (2002), The current system in the Yellow and East China seas, *J. Oceanogr.*, *58*(1), 77–92, doi:10.1023/A:1015876701363.

Latif, M. (2006), On North Pacific multidecadal climate variability, *J. Clim.*, *19*, 2906–2915, doi:10.1175/JCLI3719.1.

Levitus, S., J. I. Antonov, J. Wang, T. L. Delworth, K. W. Dixon, and A. J. Broccoli (2001), Anthropogenic warming of Earth's climate system, *Science*, *292*, 267–270, doi:10.1126/science.1058154.

Lohmann, K., and M. Latif (2005), Tropical Pacific decadal variability and the subtropical-tropical cells, *J. Clim.*, *18*, 5163–5178, doi:10.1175/JCLI3559.1.

Luo, J.-J., and T. Yamagata (2001), Long-term El Nino-Southern Oscillation (ENSO)-like variation with special emphasis on the South Pacific, *J. Geophys. Res.*, *106*, 22,211–22,227, doi:10.1029/2000JC000471.

Luo, J.-J., and T. Yamagata (2002), Four decadal ocean-atmosphere modes in the North Pacific revealed by various analysis methods, *J. Oceanogr.*, *58*(6), 861–876, doi:10.1023/A:1022831431602.

Luo, J.-J., S. Masson, S. Behera, P. Delecluse, G. Gualdi, A. Navarra, and T. Yamagata (2003), South Pacific origin of the decadal ENSO-like variation as simulated by a coupled GCM, *Geophys. Res. Lett.*, *30*(24), 2250, doi:10.1029/2003GL018649.

Luo, J.-J., S. Masson, S. Behera, and T. Yamagata (2008), Extended ENSO predictions using a fully coupled ocean-atmosphere model, *J. Clim.*, *21*, 84–93, doi:10.1175/2007JCLI1412.1.

Mantua, N. J., and S. R. Hare (2002), The Pacific decadal oscillation, *J. Oceanogr.*, *58*(1), 35–44, doi:10.1023/A:1015820616384.

Mantua, N. J., S. R. Hare, Y. Zhang, J. M. Wallace, and R. C. Francis (1997), A Pacific decadal climate oscillation with impacts on salmon, *Bull. Am. Meteorol. Soc.*, *78*, 1069–1079, doi:10.1175/1520-0477(1997)078<1069:APICOW>2.0.CO;2.

McKinnell, S. M., and W. R. Crawford (2007), The 18.6 year lunar nodal cycle and surface temperature variability in the northeast Pacific, *J. Geophys. Res.*, *112*, C02002, doi:10.1029/2006JC003671.

Mestas-Nuñez, A. M., and D. B. Enfield (1999), Rotated global modes of non-ENSO sea surface temperature variability, *J. Clim.*, *12*, 2734–2746, doi:10.1175/1520-0442(1999)012<2734:RGMONE>2.0.CO;2.

Mestas-Nuñez, A. M., and D. B. Enfield (2001), Eastern equatorial Pacific SST variability: ENSO and non-ENSO components and their climatic associations, *J. Clim.*, *14*, 391–402, doi:10.1175/1520-0442(2001)014<0391:EEPSVE>2.0.CO;2.

Mestas-Nuñez, A. M., and A. J. Miller (2006), Interdecadal variability and climate change in the eastern tropical Pacific: A review, *Prog. Oceanogr.*, *69*, 267–284, doi:10.1016/j.pocean.2006.03.011.

Minobe, S. (1997), A 50–70 year climatic oscillation over the North Pacific and North America, *Geophys. Res. Lett.*, *24*, 683–686, doi:10.1029/97GL00504.

Mizoguchi, K.-I., S. D. Meyers, S. Basu, and J. J. O'Brien (1999), Multi- and quasi-decadal variations of sea surface temperature in the North Atlantic, *J. Phys. Oceanogr.*, *29*, 3133–3144, doi:10.1175/1520-0485(1999)029<3133:MAQDVO>2.0.CO;2.

Montecinos, A., and O. Pizarro (2005), Interdecadal sea surface temperature-sea level pressure coupled variability in the South Pacific Ocean, *J. Geophys. Res.*, *110*, C08005, doi:10.1029/2004JC002743.

Moron, V., R. Vautard, and M. Ghil (1998), Trends, interdecadal and interannual oscillations in global sea-surface temperatures, *Clim. Dym.*, *14*, 545–569, doi:10.1007/s003820050241.

O'Carroll, A. G., R. W. Saunders, and J. G. Watts (2006), The measurement of the sea surface temperature by satellites from 1991 to 2005, *J. Atmos. Oceanic Technol.*, *23*, 1573–1582, doi:10.1175/JTECH1934.1.

Overland, J. E., and R. W. Preisendorfer (1982), A significance test for principal components applied to a cyclone climatology, *Mon. Weather Rev.*, *110*, 1–4, doi:10.1175/1520-0493(1982)110<0001:ASTFPC>2.0.CO;2.

Philander, S. G. H. (1990), *El Niño, La Niña and the Southern Oscillation*, 289 pp., Academic, San Diego, Calif.

Power, S., F. Tseitkin, V. Mehta, B. Lavery, S. Torok, and N. Holbrook (1999), Decadal climate variability in Australia during the twentieth century, *Int. J. Climatol.*, *19*, 169–184, doi:10.1002/(SICI)1097-0088(199902)19:2<169::AID-JOC356>3.0.CO;2-Y.

Rayner, N. A., P. Brohan, D. E. Parker, C. K. Folland, J. J. Kennedy, M. Vanicek, R. J. Ansell, and S. F. B. Tett (2006), Improved analysis of changes and uncertainties in sea surface temperature measured in situ since the mid-nineteenth century, *J. Clim.*, *19*, 446–469, doi:10.1175/JCLI3637.1.

Rodgers, K., P. Friederichs, and M. Latif (2004), Tropical Pacific decadal variability and its relation to decadal modulations of ENSO, *J. Clim.*, *17*, 3761–3774, doi:10.1175/1520-0442(2004)017<3761:TPDVAI>2.0.CO;2.

Smith, T. M., R. W. Reynolds, T. C. Peterson, and J. Lawrimore (2008), Improvements to NOAA's historical merged land-ocean surface temperature analysis (1880–2006), *J. Clim.*, *21*, 2283–2295, doi:10.1175/2007JCLI2100.1.

Sutton, R. T., and M. R. Allen (1997), Decadal predictability of North Atlantic sea surface temperature and climate, *Nature*, *388*, 563–567, doi:10.1038/41523.

Tourre, Y. M., B. Rajagoplan, Y. Kushnir, M. Barlow, and W. B. White (2001), Patterns of coherent decadal and interdecadal climate signals in the Pacific Basin during the 20th century, *Geophys. Res. Lett.*, *28*, 2069–2072, doi:10.1029/2000GL012780.

Trenberth, K. E. (1990), Recent observed interdecadal climate changes in the Northern Hemisphere, *Bull. Am. Meteorol. Soc.*, *71*, 988–993, doi:10.1175/1520-0477(1990)071<0988:ROICCI>2.0.CO;2.

Trenberth, K., and J. Hurrell (1994), Decadal atmosphere-ocean variations in the Pacific, *Clim. Dym.*, *9*, 303–319, doi:10.1007/BF00204745.

Vazquez, J., K. Perry, and K. Kilpatrick (1998), *NOAA/NASA AVHRR Oceans Pathfinder Sea Surface Temperature Data Set User's Reference Manual Version 4.0*, 83 pp., Jet Propul. Lab., Pasadena, Calif.

Vimont, D. J. (2005), The contribution of the interannual ENSO cycle to the spatial pattern of ENSO-like decadal variability, *J. Clim.*, *18*, 2080–2092, doi:10.1175/JCLI3365.1.

White, W. B., and Y. M. Tourre (2003), Global SST/SLP waves during the 20th century, *Geophys. Res. Lett.*, *30*(12), 1651, doi:10.1029/2003GL017055.

Woodruff, S. D., H. F. Diaz, J. D. Elms, and S. J. Worley (1998), COADS release 2 data and metadata enhancements for improvements of marine surface flux fields, *Phys. Chem. Earth*, *23*, 517–527, doi:10.1016/S0079-1946(98)00064-0.

Worley, S. J., S. D. Woodruff, R. W. Reynolds, S. J. Lubker, and N. Lott (2005), ICOADS release 2.1 data and products, *Int. J. Climatol.*, *25*, 823–842, doi:10.1002/joc.1166.

Wu, L., Z. Liu, R. Gallimore, R. Jacob, D. Lee, and Y. Zhong (2003), Pacific decadal variability: The tropical Pacific mode and the North Pacific mode, *J. Clim.*, *16*(8), 1101–1120, doi:10.1175/1520-0442(2003)16<1101:PDVTTP>2.0.CO;2.

Zhang, X., J. Sheng, and A. Shabbar (1998), Modes of interannual and interdecadal variability of Pacific SST, *J. Clim.*, *11*, 2556–2569, doi:10.1175/1520-0442(1998)011<2556:MOIAIV>2.0.CO;2.

Zhang, Y., J. M. Wallace, and D. S. Battisti (1997), ENSO-like interdecadal variability: 1900–93, *J. Clim.*, *10*, 1004–1020, doi:10.1175/1520-0442(1997)010<1004:ELIV>2.0.CO;2.

B. Chapron, Department of Physical and Space Oceanography, IFREMER, Center of Brest, BP 70, F-29280 Plouzané, France.

G. Chen, Y. Han, J. Ma, and B. Shao, Department of Marine Technology, College of Information Science and Engineering, Ocean University of China, 238 Songling Rd., Qingdao 266100, China. (gechen@public.qd.sd.cn)